Hydrological modeling in swelling/shrinking peat soils

M. Camporese,[1,2] S. Ferraris,[3] M. Putti,[4] P. Salandin,[1] and P. Teatini[4]

Received 14 August 2005; revised 3 February 2006; accepted 3 March 2006; published 27 June 2006.

[1] Peatlands respond to natural hydrologic cycles of precipitation and evapotranspiration with reversible deformations due to variations of water content in both the unsaturated and saturated zone. This phenomenon results in short-term vertical displacements of the soil surface that superimpose to the irreversible long-term subsidence naturally occurring in drained cropped peatlands because of bio-oxidation of the organic matter. These processes cause changes in the peat structure, in particular, soil density and void ratio. The consequential changes in the hydrological parameters need to be incorporated in water flow dynamical models. In this paper, we present a new constitutive relationship for the soil shrinkage characteristic (SSC) in peats by describing the variation of porosity with moisture content. This model, based on simple physical considerations, is valid for both anisotropic and isotropic three-dimensional peat deformations. The capability of the proposed SSC to accurately describe the deformation dynamics has been assessed by comparison against a set of laboratory experimental results recently published. The constitutive relationship has been implemented into a Richards' equation–based numerical code and applied for the simulation of the peat soil dynamics as observed in a peatland south of the Venice Lagoon, Italy, in an ad hoc field experiment where the relevant parameters are continuously measured. The modeling results match well a large set of field data encompassing a period of more than 50 days and demonstrate that the proposed approach allows for a reliable reproduction of the soil vertical displacement dynamics as well as the hydrological behavior in terms of, for example, water flow, moisture content, and suction.

Citation: Camporese, M., S. Ferraris, M. Putti, P. Salandin, and P. Teatini (2006), Hydrological modeling in swelling/shrinking peat soils, *Water Resour. Res.*, *42*, W06420, doi:10.1029/2005WR004495.

1. Introduction

[2] Histosols (organic soils) are defined by the presence of a large organic matter fraction (>50% according to the U.S. soil taxonomy system) and they are usually termed "peat" when fibrous plant remains are still visible [*Galloway et al.*, 1999]. Significant changes in land surface elevation are often observed in peatlands. Two different contributions to the overall displacements can be recognized [*Schothorst*, 1977]: irreversible long-term subsidence due to bio-oxidation of the organic matter and short time reversible swelling/shrinkage phenomena due to changes in water content. The former process, typical of drained peatlands, is very important in temperate and tropical climates, where subsidence rates can reach values of up to a few centimeters per year [*Deverel and Rojstaczer*, 1996; *Wösten et al.*, 1997]. On the other hand, reversible displacements occur mainly in response to drying/wetting or freeze/thaw cycles [*Ingram*, 1983]. Drier periods cause the occurrence of stronger matrix suction in the unsaturated zone, inducing peaks of the bulk density and resulting in a decrease of pore volume (shrinkage), while lowering of the water table induces a saturated peat compression as the effective stresses increase [*Price*, 2003]. Depending on the ratio between the thickness of the unsaturated and saturated zones, shrinkage and compression may have different relative importance, even though it is recognized that the rate of volume change in the unsaturated zone is greatest [*Price*, 2003; *Kennedy and Price*, 2005]. Experimental evidence shows that the high compressibility of peat may yield volumetric changes up to 10 times larger than in swelling clay soils [*Hobbs*, 1986]. Fibrous and poorly decomposed peatlands may experience displacements induced by water content changes of the order of 0.1 m [*Price and Schlotzhauer*, 1999], whereas seasonal movements are relatively small ($\approx$0.01 m) in amorphous organic soils [*Deverel and Rojstaczer*, 1996]. The latter case is typical of histosols subject to intensive agriculture. In these cases, vertical profiles usually exhibit a deep layer of undecomposed peat overlain by an amorphous partially mineralized soil, which may vary in thickness between few centimeters and half a meter, depending on local agricultural practices. The shallow layer often coincides with the unsaturated zone, and may be subject to swelling/shrinking deformations with magnitudes comparable with the rates of irreversible

[1]Department of Hydraulic, Maritime, Environmental and Geotechnical Engineering, University of Padua, Padua, Italy.
[2]Now at Centre Eau, Terre and Environnement, Institut national de la recherche scientifique, University of Quebec, Quebec, Quebec, Canada.
[3]Department of Agricultural, Forestry and Environmental Economics and Engineering, University of Turin, Grugliasco, Italy.
[4]Department of Mathematical Methods and Models for Scientific Applications, University of Padua, Padua, Italy.

0043-1397/06/2005WR004495$09.00

subsidence due to the long-term organic matter oxidation. Over short time periods (few years) the superposition of the two phenomena may interfere with measurements of irreversible subsidence, so that the understanding of the long-term behavior needs to take into consideration possible deviations from the general trend due to the reversible deformations.

[3] The sequence of swelling and shrinkage events, known also as "mire breathing", is a key issue for the hydrological and ecological dynamics of peatlands [*Price and Whitehead*, 2001] as it produces short-term changes in the pore structure, and thus on the density and hydraulic properties of peat soils [*Price and Schlotzhauer*, 1999]. For these reasons, not only the porosity but also the entire set of retention and relative conductivity curves, together with saturated hydraulic conductivity and water storativity, must be considered to vary dynamically with changes of water content [*Schlotzhauer and Price*, 1999]. Hydrological models of peat soils must incorporate a description of volume changes as a function of moisture dynamics to avoid potentially large errors in the prediction of water fluxes [*Smiles*, 2000; *Kennedy and Price*, 2004].

[4] A number of swelling/shrinking models of peat soils have been proposed in the last few years [*Pyatt and John*, 1989; *Price*, 2003; *Oleszczuk et al.*, 2003; *Hendriks*, 2004; *Kennedy and Price*, 2004, 2005]. *Pyatt and John* [1989] propose a two-stage model expressing the shrinkage of well-decomposed saturated peats in terms of specific volume and gravimetric water content changes. A threshold value of the gravimetric water content separates the stage of one-dimensional vertical deformation from the stage where the peat experiences isotropic three-dimensional deformations with the development of cracks in the porous medium. An attempt to apply this model to reproduce the data set collected from a bog in Québec, Canada, did not provide satisfactory results, probably because of the effects due to bubbles of gaseous methane in the soil [*Price*, 2003].

[5] Shrinkage characteristic curves are commonly described by means of empirical expressions relating void and moisture ratios. These parameters are preferred with respect to, e.g., water content and porosity, because they refer to the volume of solids, which, differently from total volume, is not subject to dynamical changes [*Bronswijk*, 1988]. Several laboratory experiments on European peats show that the shrinkage characteristic (SSC) is significantly different from that of clay soils [*Van den Akker and Hendriks*, 1997; *Oleszczuk et al.*, 2003; *Hendriks*, 2004]. According to *Hendriks* [2004], three phases can be distinguished during peat drying. A near-normal shrinkage phase occurs when the soil volume decreases at approximately the same rate of moisture content and the peat matrix remains close to saturation. Subnormal shrinkage takes place when moisture loss exceeds volume change and the soil becomes definitely unsaturated, with air entering the larger pores, while the smaller pores in the organic fibers remain water filled. Finally, supernormal shrinkage develops when the volume reduction is greater than moisture loss. During this phase, also the small pores dry and the matrix collapses to its minimum volume as moisture content approaches zero. Note that especially at these low water contents, clays display a notably different behavior, being characterized by a phase of zero volume change [*Hendriks*, 2004]. A three-line constitutive model has been proposed by *Oleszczuk et al.* [2003] as a first attempt to reproduce this characteristic behavior. In this model six constitutive constants must be determined by fitting laboratory data. A more complex expression has been developed by *Hendriks* [2004] by employing a moisture-void ratio relationship that depends again on six parameters: moisture ratio at saturation and at the transition from the near-normal to the subnormal phase, residual void ratio, i.e., void ratio at zero moisture content, and three fitting parameters. Such a large number of degrees of freedom entails an accurate description of the overall deformation process, but requires the availability of specific laboratory data and the estimation of their representativeness at the field scale.

[6] A different approach is followed by *Kennedy and Price* [2004, 2005], who developed a conceptual model that considers several hydrological parameters as functions of peat density and, consequently, of effective stresses. This model, which allows the simulation of reversible deformations in both the saturated and unsaturated zone, is based on Terzaghi's theory of consolidation [*Terzaghi*, 1943], extending the validity of the effective stress principle to the unsaturated zone. Several processes are simultaneously taken into account in both zones: shrinkage and temporally variable retention curves are considered in the partially saturated soil portion, while, below the water table, primary consolidation, secondary compression, and variable hydraulic conductivity are taken into account. Again, the values of a large number of both physically based and empirical parameters need to be estimated from laboratory experiments and in situ tests. Application of this model and results from field observations at the Lac-Saint-Jean cutover bog, Québec, show that shrinkage in the unsaturated zone and compression below the water table represent 55–59% and 38–41% of the total soil surface elevation change, respectively. The shrinkage rates are larger than compression rates, even if the relative importance is similar, since the considered unsaturated layers represent a small proportion ($\leq$30%) of the overall aquifer thickness [*Kennedy and Price*, 2005].

[7] The objective of our study is the development of a physically based constitutive model of swelling and shrinkage in peat soils, which is characterized by a limited number of parameters, but at the same time is capable of accurately describing three-dimensional anisotropic deformations in the unsaturated zone. We develop a two-parameter SSC relationship by extending the capabilities of the model proposed by *Pyatt and John* [1989]. The peat soil moisture is linked to the void ratio, which in turn affects the thickness (soil surface elevation) of the peat layer. The developed SSC is implemented in a simulation code of groundwater flow in variably saturated soils and applied to a set of field observations collected in a peat site located south of the Venice Lagoon, Italy [*Gambolati et al.*, 2005]. The application of the model over a 2-month period, containing a few rainfall events, supports the validity of the proposed approach.

2. Model Formulation

2.1. Constitutive Relationship for Saturated Peat Soils

[8] Swelling/shrinkage of peat can be described by constitutive relationships relating volume variations to moisture

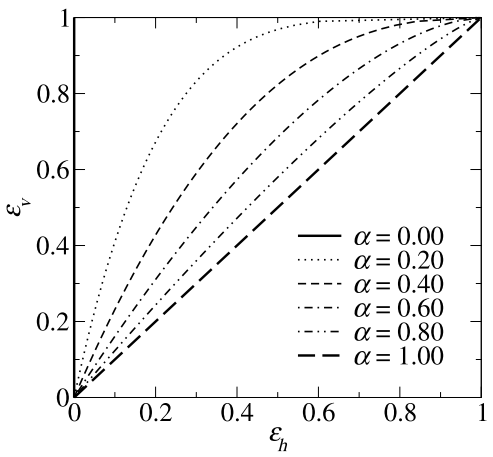

Figure 1. Vertical deformation ($\varepsilon_v = 1 - \ell/\ell_0$) versus horizontal deformation ($\varepsilon_h = 1 - \ell'/\ell_0$) for different values of the exponent α used in the proposed power law.

content changes, i.e., the soil shrinkage characteristics. We consider a volume V of soil, expressed as $V = V_s + V_v$, where V_s is the volume of the solid fraction and V_v the volume of the voids. The voids can be partially or totally filled by water, and hence the water volume fraction V_w can be smaller or at most equal to V_v. We denote by M_s and M_w the mass of the solid and water fractions, respectively. Experimental results reported by *Pyatt and John* [1989] show that during drying, the volume of a saturated cube of peat decreases linearly with the gravimetric water content $\Theta = M_w/M_s$. The specific volume ($v = V/M_s$) can thus be expressed as $v(\Theta) = \Theta\ v_w + v_s$, where $v_w = V_w/M_w$ is the specific volume of water and $v_s = V_s/M_s$ is the specific volume of solids. The relationship $v(\Theta)$ is called the saturation line. In these conditions, shrinkage occurs in two stages. One-dimensional vertical displacements take place for a gravimetric water content above a threshold value Θ_0 (stage 1). Below this value, cracks appear in the soil layer and a fully three-dimensional isotropic deformation pattern is considered (stage 2). To exemplify this situation, assume that a peat volume of initial height ℓ_i is characterized by a gravimetric water content Θ_i and is subject to drying. During stage 1, the peat shrinks vertically in the same proportion as the specific volume decreases along the saturation line. Thus, denoting by Θ the current water content, *Pyatt and John* [1989] propose

$$\frac{\ell}{\ell_i} = \frac{v}{v_i} = \frac{\Theta v_w + v_s}{\Theta_i v_w + v_s} \quad \text{for } \Theta_0 \le \Theta \le \Theta_i, \tag{1}$$

where ℓ is the vertical height of the current volume. At the inception of cracks, deformations become isotropic and a cube of initial volume ℓ_0^3 will shrink to ℓ^3 following the relationship [*Pyatt and John*, 1989]:

$$\left(\frac{\ell}{\ell_0}\right)^3 = \frac{v}{v_0} = \frac{\Theta v_w + v_s}{\Theta_0 v_w + v_s} \quad \text{for } 0 \le \Theta \le \Theta_0. \tag{2}$$

In a more general situation peat may be partially saturated and anisotropic three-dimensional deformations may occur. Under such conditions the above model needs to be extended appropriately.

2.2. Extension to the Unsaturated Zone

[9] We describe here our developments for extending the previous model to unsaturated peats undergoing three-dimensional anisotropic deformations. Following the developments proposed by *Bronswijk* [1990] for clays, we postulate that the peat volume shrinks following an intermediate behavior between the two cases given by equations (1) and (2). This intermediate condition is characterized by a gravimetric water content smaller than the threshold value Θ_0, which can be considered as the threshold below which relationship (1) ceases to be valid. In this situation, three-dimensional anisotropic deformations need to be taken into account. To this aim, let ℓ' be the horizontal dimension after shrinkage, equal to ℓ only in the isotropic case. We then use a power law to describe the relationship between horizontal and vertical relative displacements, $(\ell'/\ell_0) = (\ell/\ell_0)^\alpha$ (see Figure 1), and derive the following expression:

$$\left(\frac{\ell'}{\ell_0}\right)^2 \frac{\ell}{\ell_0} = \left(\frac{\ell}{\ell_0}\right)^{2\alpha+1} = \frac{v}{v_0} = \frac{\Theta v_w + v_s}{\Theta_0 v_w + v_s}, \tag{3}$$

with α a nonnegative parameter. The shrinkage geometry factor r_s of *Bronswijk* [1990] and *Oleszczuk et al.* [2003] is recovered as $r_s = 2\alpha + 1$. For $\alpha = 1$ the isotropic case is considered and $r_s = 3$. For $\alpha = 0$, $r_s = 1$ and $\ell' = \ell_0 = const$, taking into account only one-dimensional vertical deformations. A value of $\alpha > 1$ ($r_s > 3$) corresponds to an event in which significant cracks form [*Pyatt and John*, 1989; *Oleszczuk et al.*, 2003]. Values of r_s ranging between 1 and 3 identify a process of three-dimensional anisotropic soil deformation not included in the model of *Pyatt and John* [1989].

[10] Let us consider a peat volume undergoing three-dimensional anisotropic deformations and inserted in a soil layer. We assume that no or negligibly small cracks occur, i.e., $0 \le \alpha < 1$ or equivalently $1 \le r_s < 3$, a situation encountered in our cropped peatlands [*Camporese et al.*, 2004; *Camporese*, 2006]. Note that the latter hypothesis allows us to consider the soil as a continuous medium so that a relationship between the specific volume and the gravimetric water content of the peat layer can be determined. We make here the assumption that the horizontal scale of the peat layer is much larger than its thickness. This allows us to consider the peat volume as inserted into a semi-infinite medium bounded from above by the ground surface. Under these conditions, because of the horizontal symmetry of the domain and further assuming that the horizontal components of the water pressure gradients are small with respect to the vertical components, the horizontal deformation translates into a pore structure rearrangement, causing a variation of the void ratio $e = V_v/V_s$, and contributing to the total vertical displacement [*Gambolati*, 1974]. Indicating with v^* the specific volume in the peat layer, expressed as

$$v^* = \frac{\ell \ell_0^2}{M_s}, \tag{4}$$

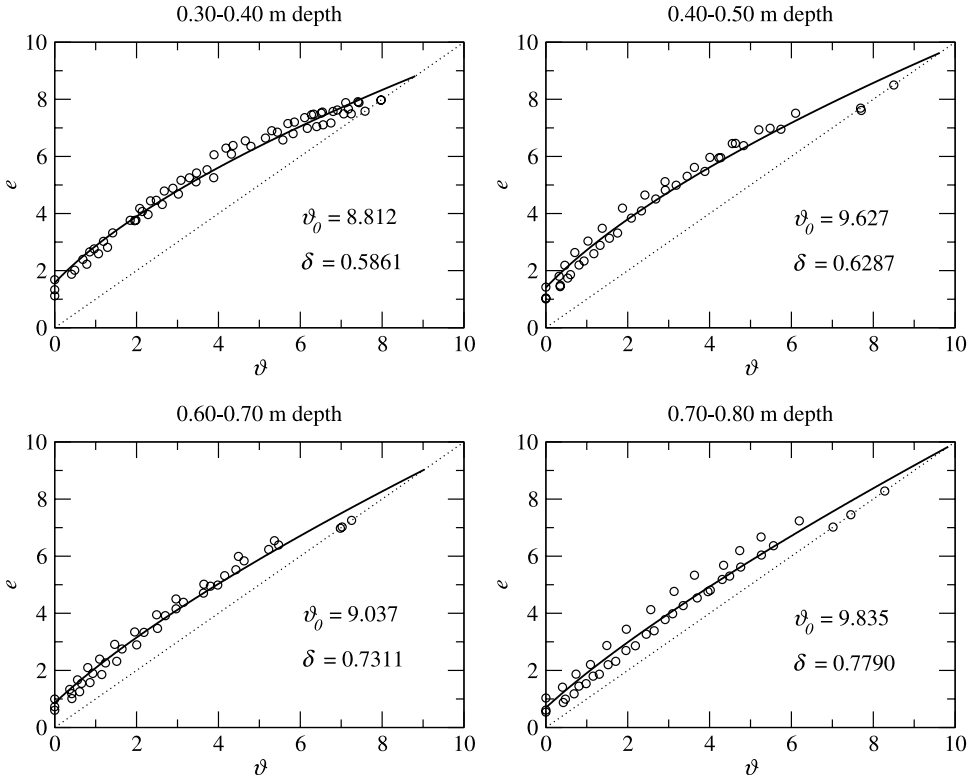

Figure 2. Fitting of the proposed constitutive model (equation (9), solid lines) to the experimental data (○) collected by *Oleszczuk et al.* [2003] at various depths. Dotted lines represent the saturation line.

and using equation (3), we obtain

$$v^* = (\Theta_0 v_w + v_s)^{1-\delta}(\Theta v_w + v_s)^{\delta}, \tag{5}$$

where $\delta = 1/(2\alpha + 1) = 1/r_s$. The final version of the proposed model is obtained by reformulating equation (5) in terms of volumetric quantities. The specific volume inside a layer can be expressed as a function of the void ratio:

$$v^* = v_s(1 + e), \tag{6}$$

and the gravimetric moisture content can be defined as a function of the moisture ratio $\vartheta = V_w/V_s$:

$$\Theta = \frac{\vartheta v_s}{v_w}. \tag{7}$$

Substituting v^* and Θ in equation (5), the shrinkage characteristic curve of the peat can be written as

$$e = (\vartheta_0 + 1)^{1-\delta}(\vartheta + 1)^{\delta} - 1, \tag{8}$$

where ϑ_0 is the moisture ratio corresponding to the threshold gravimetric water content Θ_0. For $\delta = 1$, the proposed model coincides with the saturation line $e = \vartheta$, written in terms of volumetric quantities. For values $\delta \neq 1$ the intersection between equation (8) and the saturation line occurs at $\vartheta = \vartheta_0$. When the moisture ratio is greater than the threshold value ϑ_0 and $\delta \neq 1$ the shrinkage curve lies below the saturation line. This situation has no physical meaning as it would yield $V_v < V_w$. Thus equation (8) must be considered valid only for $\vartheta \leq \vartheta_0$. Laboratory evidence [*Pyatt and John*, 1989] show that for large moisture ratios and saturated soil, the swelling/shrinkage line follows the saturation line, corresponding to the stage 1 behavior ($\delta = 1$) as described by equation (1). The threshold moisture ratio ϑ_0 (and hence the corresponding gravimetric water content Θ_0) can then be interpreted as the value above which peat is totally saturated. The final model can then be written as

$$e = \begin{cases} (\vartheta_0 + 1)^{1-\delta}(\vartheta + 1)^{\delta} - 1 & \text{if } \vartheta \leq \vartheta_0 \\ \vartheta & \text{if } \vartheta > \vartheta_0 \end{cases}. \tag{9}$$

[11] To verify the capability of the proposed constitutive model in reproducing actual peat shrinkage behavior, the model results are compared against the data of *Oleszczuk et al.* [2003], who analyzed peat samples collected at different depths taking into account the in situ loading conditions. Figure 2 shows the shrinkage curves given by (9) adapted to the different data sets by calibrating the values of δ and ϑ_0. A satisfactory match is obtained with values of δ that increase linearly with depth. At higher loading conditions the shrinkage curve tends to collapse onto the saturation line. This behavior is related to the stress rise due to the overburden load that is accounted for in the laboratory experiments [*Oleszczuk et al.*, 2003] and is consistent with data by *Bronswijk* [1990], who observed a large difference in the measured values of the shrinkage geometry factor between loaded and unloaded clay samples. The value of ϑ_0 is always close to 9, with a fluctuation that is small

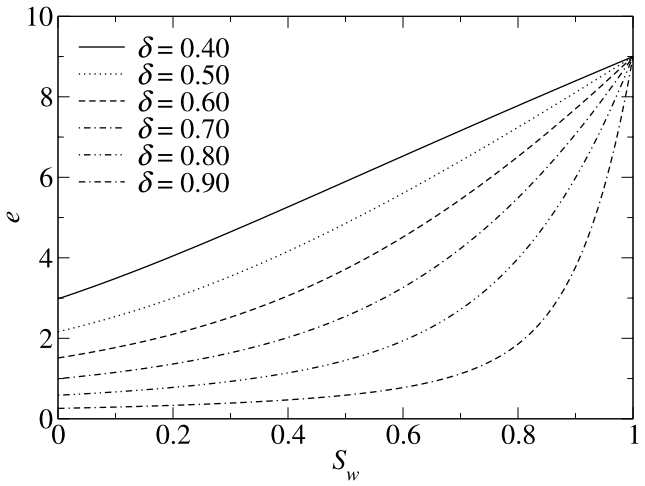

Figure 3. Relationship between void ratio and water saturation according to equation (14), with $\vartheta_0 = 9.0$.

compared to the total range of ϑ variability, showing the robustness of our model formulation.

2.3. Implementation of the Shrinkage Model in Richards' Equation

[12] The flow equation for variably saturated porous media, also known as Richards' equation, can be written in terms of pressure head ψ as

$$\sigma \frac{\partial \psi}{\partial t} = \nabla \cdot [K_s K_r \nabla(\psi + z)] + q, \tag{10}$$

where $\sigma(S_w)$ is the general storage term (also known as specific moisture capacity), with $S_w(\psi) = V_w/V_v$ being the water saturation, t is time, ∇ is the spatial gradient operator, K_s is the saturated hydraulic conductivity, $K_r(S_w)$ is the relative hydraulic conductivity, z is the vertical coordinate, positive if directed upward, and q represents the source or sink term. The model is completed by appropriate boundary and initial conditions and by the retention curves $S_w(\psi)$ and $K_r(S_w)$, which can be given following any relationship available in literature [see, e.g., *Brooks and Corey*, 1964; *van Genuchten*, 1980].

[13] The general storage term is written as the sum of two contributions:

$$\sigma = S_w \frac{\partial \phi}{\partial \psi} + \phi \frac{\partial S_w}{\partial \psi} = S_w S_s + \phi \frac{\partial S_w}{\partial \psi}, \tag{11}$$

where $S_s = \partial\phi/\partial\psi$ is the elastic storage coefficient, that takes into account the elastic compressibility of the porous matrix, and $\phi = V_v/V$ is the porosity of the medium. When dealing with mineral soils in unsaturated flow conditions, the term $S_w S_s$ can be often neglected as compared to $\phi \partial S_w/\partial\psi$. The presence of the elastic storage coefficient in σ becomes important in saturated conditions, where $\partial S_w/\partial\psi$ vanishes. In organic soils however, where volume changes due to soil moisture variations need to be taken into account, porosity varies with space and time as a function of water saturation and the elastic storage coefficient may not be negligible [*Dasberg and Neuman*, 1977; *Price and Schlotzhauer*, 1999]. Taking into consideration the changes of ϕ with S_w, we can write

$$\sigma = S_w \frac{\partial \phi}{\partial S_w} \frac{\partial S_w}{\partial \psi} + \phi \frac{\partial S_w}{\partial \psi}. \tag{12}$$

The porosity ϕ and the water saturation S_w are related to the void ratio e by

$$\phi = \frac{e}{1+e} \qquad S_w = \frac{\vartheta}{e(\vartheta)}. \tag{13}$$

For the case $S_w < 1$, i.e., $\vartheta < \vartheta_0$, substitution of the second equation of (13) into (8) yields the following implicit expression for $e(S_w)$:

$$e(S_w) = (\vartheta_0 + 1)^{1-\delta}(eS_w + 1)^{\delta} - 1. \tag{14}$$

The behavior of this function is shown in Figure 3 for values of δ ranging between 0.4 and 0.9. All the curves show a monotonic increase with saturation and coincide for the limiting value $e = \vartheta_0$. As δ tends to 1 the function approaches the vertical line $S_w = 1$, i.e., fully saturated condition.

[14] Using the first of (13), the expression of $\partial\phi/\partial S_w$ can be determined as

$$\frac{\partial \phi}{\partial S_w} = \left(\frac{1}{1+e}\right)^2 \frac{\partial e}{\partial S_w}. \tag{15}$$

The formula for $\partial e/\partial S_w$ can be obtained from equation (14), yielding

$$\frac{\partial e}{\partial S_w} = \frac{(\vartheta_0 + 1)^{1-\delta}\delta(eS_w + 1)^{\delta-1} e}{1 - (\vartheta_0 + 1)^{1-\delta}\delta(eS_w + 1)^{\delta-1} S_w}. \tag{16}$$

Using (12), (14), and (16), the following formulation of the general storage term for unsaturated swelling peat is derived

$$\sigma = \frac{e}{1+e} \frac{\partial S_w}{\partial \psi} \times \left[\frac{\delta(eS_w + 1)^{-1}}{1/S_w - (\vartheta_0 + 1)^{1-\delta}\delta(eS_w + 1)^{\delta-1}} + 1 \right]. \tag{17}$$

Developing the products in equation (17) and comparing with (11), we can determine an expression that can be interpreted as an elastic storage coefficient for partially saturated peat:

$$S_{uns} = \frac{\delta(eS_w + 1)^{-1}}{1 - (\vartheta_0 + 1)^{1-\delta}\delta(eS_w + 1)^{\delta-1} S_w} \times \left(\frac{e}{1+e} \frac{\partial S_w}{\partial \psi} \right). \tag{18}$$

This equation shows that S_{uns} depends on the pressure head, both through the dependence of e on S_w and of S_w and its derivative on ψ. Note that our formulation closely follows the work of *Philip* [1969] for swelling media, where the storage coefficient is expressed as a function of e instead of ϕ since the void ratio is related to V_s, a quantity that can be assumed constant at short timescales. Consistently with the validity range of (14), equations (17) and (18) apply only to the unsaturated zone. For peat soils in fully saturated conditions, S_w is equal to one, and equation (12) reduces to

the classical elastic storage coefficient S_s. In this specific application S_s is kept constant if $S_w = 1$.

2.4. Numerical Solution

[15] The above formulation of the modified storage term has been implemented in a finite element code that discretizes Richards' equation by means of linear elements in space and backward Euler in time. The nonlinear system of equations, which arises at each time step from the temporal and spatial discretization, is solved using the Picard technique: linearization is achieved by evaluation of the nonlinear terms at the previous iteration level [*Paniconi and Putti*, 1994]. Because of the nonlinear form of (17), its actual value is updated within each Picard iteration as well [*Camporese et al.*, 2004; *Camporese*, 2006].

[16] For each node of the discretization, the vertical relative displacement of the associated layer (i.e., the ratio between current and initial thickness) is computed at each time step as

$$\frac{\ell(t)}{\ell(0)} = \left[\frac{1+e(t)}{1+e(0)}\right]^{\delta}, \tag{19}$$

where $t = 0$ refers to an initial stage of zero soil deformation. Equation (19) derives from (6), where the ratio $v^*(t)/v^*(0)$ is expressed by means of (3) as a function of $\ell(t)/\ell(0)$. According to the anisotropic behavior discussed in Section 2.2, the use of a value of δ different from 1 is necessary to "extract" the vertical component from the volumetric deformation, which is expressed in terms of void ratio changes. The numerical integration of (19) over the total depth of the soil domain provides the actual thickness of the peat column, from which the soil surface displacements can be evaluated. Using this approach, the unsaturated zone contributes to the total deformation through equation (18), while compression in the saturated zone is not taken into account in the present application. From the experimental point of view, there is controversial evidence in the literature [*Price*, 2003; *Kennedy and Price*, 2005] on the relative importance of the deformation in the unsaturated and saturated soil portions. In our case we do not possess any field record on the deformation of the saturated peat. Since our field experiment is similar to the "2-year" and "7-year abandoned" study sites of *Price* [2003], we accept his observation of a contribution of the saturated zone of less than 5%.

3. Application Example

3.1. Site Description

[17] The model has been applied to the experimental data set collected at the Zennare Basin, a drained cropped peatland located south of the Venice Lagoon, Italy, where land subsidence due to organic soil oxidation on the order of 1.5–2 m has been observed over the past 70 years. This occurrence presently jeopardizes the sustainable development of this portion of the Venice territory that lies almost entirely below sea level, down to as much as −4 m with respect to msl [*Gambolati et al.*, 2006]. The basin is artificially drained by a pumping station and a fine network of small ditches is used to maintain an average water table depth varying between 0.3 and 0.5 m.

[18] The study of the relationship between the hydrological regime and the subsidence rates is conducted by means of a field experimental project operating since the end of 2001. The field site is located within a rectangular plot of size 30 m × 200 m with a 1.5 m thick peat layer and drained laterally by ditches [*Fornasiero et al.*, 2003]. The organic soil is formed from the decomposition of reeds (Phragmites spp.). The complete description of the project and of all the instruments, together with pictures of the field sites, can be found on the Web at http://voss.dmsa.unipd.it. Differently from the experiments by *Glaser et al.* [2004] and *Kellner et al.* [2005], methane production in the Zennare peat is negligible (unpublished data, 2003), since environmental conditions are mainly aerobic. Thus possible horizontal displacements due to gas bubble effects [*Glaser et al.*, 2004] are negligible. The following devices were installed and operated for more than 2 years [*Fornasiero et al.*, 2003]: (1) a tilting bucket pluviometer with a sensitivity of 0.2 mm, (2) a nondirectional anemometer with an accuracy of 0.25 m/s, (3) two piezometers, one located within the test site and the other close to the adjacent ditch, both made from 3 m long PVC pipe of 5.08 cm diameter and instrumented with an atmosphere-compensated pressure transducer characterized by a measuring range of 0–300 mbar and an accuracy of ±1.5 mbar, (4) five tensiometers to measure the capillary pressure, inserted at a 45° slope so that the ceramic cups are all located along the same vertical line, with a depth interval of 15 cm down to 75 cm; the measurement range of the electronic pressure sensor is from −1000 to 850 hPa with an accuracy of ±0.2 hPa, (5) six three-wire time domain reflectometry (TDR) probes for soil moisture content measurement (accuracy ±0.02 m^3/m^3), 15 cm long, inserted horizontally along the same vertical of the tensiometers, at depths of 10, 20, 30, 45, 60, and 75 cm, and connected to a multiplexer, and (6) five soil temperature sensors at 1, 5, 15, 30, and 100 cm depths with a measurement range between −15°C and 50°C and an accuracy of ±0.1°C. As suggested by *Deverel and Rojstaczer* [1996], ground surface displacement is monitored by an extensometer: three displacement transducers, characterized by a measurement range of 0–25 mm and an accuracy of ±0.125 mm, are attached at one end to a steel tripod anchored on three piles set into the ground to a depth of 12 m where an overconsolidated clay layer is located. The other end is connected to the land surface through a 0.5 cm thick, 10 × 10 cm aluminum plate resting on the soil. The triangular steel structure, with sides of approximately 2 m, has been designed to be as light as possible but with a negligible deformation with respect to the expected subsidence rate when loaded with the force exerted by the displacement transducers (2.5 kg each) and by a thermal excursion of 40°C. All analog sensors are connected to a data logger and sampled hourly, so that a large data set is available for the study of the hydrological and swelling/shrinking peat dynamics. Only the multiplexed Tektronix 1502C TDR data are collected at bihourly intervals, from a different logging system. It is worth recalling that TDR provides measurements of the bulk dielectric permittivity K_b, that can subsequently be related to the volumetric water content θ [*Topp et al.*, 1980]. The latter is defined as V_w/V and is related to ϑ by the function $\vartheta = \theta(1 + e)$. The conversion from K_b to θ depends on the soil electric

characteristics. For peats, several calibration functions have been proposed in the literature. Since a specific TDR calibration curve is not currently available for the Zennare peat, we have elected to use the function proposed by *Myllys and Simojoki* [1996], developed for cropped peat soils and thus similar to the conditions of our basin.

[19] A preliminary analysis of the collected measurements shows that significant reversible peat volume changes are caused by variation of soil moisture. Peat swelling has been noticed after every rainfall event. The swelling dynamics is very rapid after a precipitation event, while shrinkage progresses at a slower rate, closely following the water table decrease and exhibiting a timescale from few hours to few weeks [*Teatini et al.*, 2004].

3.2. Simulation Setup

3.2.1. Model Domain

[20] A 1.5 m thick peat column with a horizontal square surface of side 0.2 m is used to simulate the recorded displacements and hydrological data. The domain surface is discretized by 32 right-angled triangles (5 × 5 nodes) that are replicated vertically 16 times to form 15 layers yielding a three-dimensional mesh of 1440 tetrahedral finite elements and 400 nodes. The topmost 10 layers have a thickness equal to 0.05 m. The subsequent two layers are 0.10 m thick and are followed by one 0.20 m and two 0.30 m thick layers.

3.2.2. Boundary and Initial Conditions

[21] Reproduction of the physical environment found in the field requires that boundary conditions be prescribed as follows. The column bottom is assumed impermeable, since the peat is bounded by a thick clay formation [*Gatti et al.*, 2002]. The water table on the lateral boundaries is imposed to vary according to the groundwater levels measured by the piezometer located within the test site. Atmospheric forcing, given by the difference between actual rainfall and potential evapotranspiration (ET_0), is calculated as follows. Hourly rainfall records available from the rain gauge are complemented by daily potential evapotranspiration rates estimated by the FAO-Penman-Monteith equation, which gives the reference ET_0 values [*Allen et al.*, 1998]. Global radiation, mean air temperature, and relative humidity data required to evaluate ET_0 are taken from a nearby agrometeorological station, while wind velocity is measured by the anemometer located in the field. The dynamically variable surface boundary conditions are implemented as follows. In a typical simulation the fraction of water that remains at the surface and is not able to infiltrate into the soil is calculated by the code. The input flux values are considered "potential" infiltration or exfiltration rates, and the "actual" rates, which depend on the prevailing flux and pressure head values at the surface, are dynamically calculated by the code during the simulation [*Bixio et al.*, 2000; *Putti and Paniconi*, 2004]. In the current implementation the ponding effect produced by the fraction of water that does not infiltrate into the soil is neglected, assuming an instantaneous runoff discharge.

[22] In the unsaturated zone, initial conditions are interpolated from the ψ distribution provided by the tensiometers, and an hydrostatic profile that follows the piezometer readings is used in the saturated part of the soil column. Some preliminary tests have however demonstrated that a period of 200 hours is long enough for the system to be independent of the initial conditions, by dissipating the uncertainty on the pressure field imposed at $t = 0$.

3.2.3. Model Parameterization

[23] The integration of Richards' equation (10) with the general storage term expressed by (17) requires the determination of the constitutive relationships $S_w(\psi)$ and $K_r(S_w)$, the shrinkage curve parameters ϑ_0 and δ, and the saturated hydraulic conductivity K_s. Since partially saturated conditions generally prevail in the Zennare peatland and the saturated peat is primarily controlled by the boundary conditions described above, we are mainly focused on the unsaturated zone. Thus the value of the elastic storage coefficient for $S_w = 1$ has no influence on the model output above the water table, so that we elected to keep it constant and equal to $S_s = 5 \times 10^{-4}\ \mathrm{m}^{-1}$. The dependence of S_w on ψ and K_r on S_w for peat soils is evaluated by means of the van Genuchten model [*van Genuchten*, 1980; *Weiss et al.*, 1998]:

$$S_{we} = \frac{S_w - S_{wr}}{1 - S_{wr}} = \begin{cases} \left[\dfrac{1}{1 + (\psi/\psi_s)^n}\right]^m & \text{if } \psi < 0 \\ 1 & \text{if } \psi \geq 0 \end{cases} \tag{20}$$

$$K_r = S_{we}^{1/2}\left[1 - \left(1 - S_{we}^{1/m}\right)^m\right]^2, \tag{21}$$

where S_{we} and S_{wr} are the effective and residual water saturation, respectively, ψ_s and n are fitting parameters, and $m = 1 - 1/n$. The value of S_{wr} is calculated as the ratio between the residual volumetric water content θ_r and porosity. Since ϕ is a function of ψ, so is S_{wr}. As a consequence, our model takes into account also the temporal variability of the retention curve.

[24] Volumetric water content θ versus pressure head ψ, as collected at different depths, are shown in Figure 4. Since the uppermost tensiometers and TDR probes are placed at different depths, the values of θ at 0.15 m are calculated by linear interpolation between the measurements at 0.10 and 0.20 m. The data set points out that the retention curves vary with depth with a flattening of the function passing from 0.15 to 0.30 m. We have calibrated the Van Genuchten parameters n, ψ_s and θ_r by a best fit on the 0.15 m depth data set, where unsaturated conditions prevail. The resulting values are $n = 1.34$, $\psi_s = -0.58$ and $\theta_r = 0.22$ (see also Table 1). The experimental data shown in Figure 4 allow also the estimation of the volumetric water content corresponding to $\psi = 0$, i.e., θ_0 at the saturation limit, from which we can calculate ϑ_0. Capillary fringe, that on disturbed peat subject to oxidation can range between 0.15 and 0.25 m above the water table [*Price and Whitehead*, 2001], has no influence on the estimation of θ at the limit of saturation. At the saturation limit the value of θ_0 ranges from 0.66 at the ground surface to 0.90 at 0.60 m depth. This is consistent with the geotechnical classification of the Zennare peat [*Gatti et al.*, 2002], which shows that a fibrous peat layer of approximately 1.0 m is overlain by a shallow (0.5 m) partially decomposed peat layer. As a consequence, the corresponding value of ϑ_0 ranges from 1.96 to 9.00. The

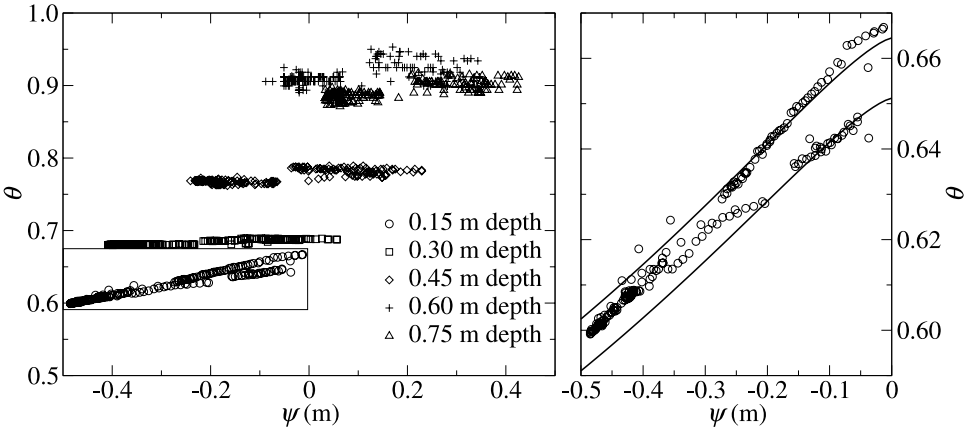

Figure 4. Volumetric water content and pressure head at various depths, as measured by TDR probes and tensiometers. On the right we show the enlargement of the data points collected at 0.15 m depth. The dual behavior of these values is likely to be related to hysteresis, with the upper circles corresponding to drainage and the lower ones to wetting. The two lines represent the range of variability of the van Genuchten retention curves for the extreme values of ϕ as calculated by the model during the entire simulation.

last two parameters, δ and K_s, have been calibrated as explained in detail in section 4.

4. Numerical Results

[25] The model has been applied over the period between 20 December 2003 and 2 February 2004. The time interval is characterized by the occurrence of two significant rainfall events, dated 28–31 December 2003 and 17–19 January 2004, with intervening dry periods. No freezing conditions occurred in this period, with the exception of short nightly low soil temperature values observed only at the surface. For this reason, it is considered as a meaningful test for verification of the model capabilities to reproduce the peat displacement and hydrological dynamics. The simulation period is divided in three phases. Phase I consists of the initialization of the model. Phase II lasts from 200 to 680 hours and is used for calibration purposes. Phase III, from 680 hours to the end of the simulated period (about 1320 hours), is used for "prediction" of the available data. Note that both phases II and III are characterized by the occurrence of a significant rainfall event. Figure 5 shows the soil temperature at a depth of 0.01 m, atmospheric forcing, and soil surface displacements recorded during the entire period.

4.1. Calibration

[26] The saturated hydraulic conductivity K_s and the swelling/shrinking model parameter δ are calibrated by fitting the measured and simulated surface displacements and pressure head profiles of phase II. The increased value of δ with depth, as observed by the data of *Oleszczuk et al.* [2003], is taken into account by means of the following linear relationship:

$$\delta(z) = \delta_{sur} + \lambda(D - z), \tag{22}$$

where δ_{sur} is the value of δ evaluated at the soil surface, D is the total column height, and λ is a calibration parameter. Calibration is performed for the two swelling/shrinkage parameters δ_{sur} and λ. The Willmott index of agreement, defined as [*Willmott*, 1948]

$$d = 1 - \frac{\sum_i (O_i - P_i)^2}{\sum_i \left(|O_i - \overline{O}| + |P_i - \overline{O}|\right)^2}, \tag{23}$$

is used to evaluate the best fit between measured and simulated quantities. In equation (23), O_i are the observed (hourly) values, P_i are the corresponding quantities computed by the model, and $\overline{O}$ is the mean of the observed values. The value for d ranges from 0, indicating no agreement, to 1, which ensures a perfect reproduction. Parameter d is more accurate than the usual coefficient of determination because it is insensitive to a number of potential additive and proportional differences between observed and predicted values [*Willmott*, 1948; *Letts et al.*, 2000]. Since at 0.75 m the soil is always in saturated conditions, only the four pressure head time series measured by the tensiometers located within the vadose zone between 0.15 and 0.60 m are taken into account. This is obtained by defining an average Willmott parameter $\overline{d}_\psi$ computed as the arithmetic average of the Willmott parameters calculated at each depth. Since the displacements are defined up to an additive constant, peat surface deformations are included by evaluating the parameter d_* for the displacement differences.

Table 1. Parameter Values Used in the Numerical Simulation of the Zennare Peatland

Parameter	Value
K_s	3×10^{-7} m/s
S_s	5×10^{-4} m^{-1}
n	1.34
θ_r	0.22
ψ_s	−0.58 m
δ_{sur}	0.35
λ	0.10 m^{-1}
$\vartheta_0(z)$	see Figure 9

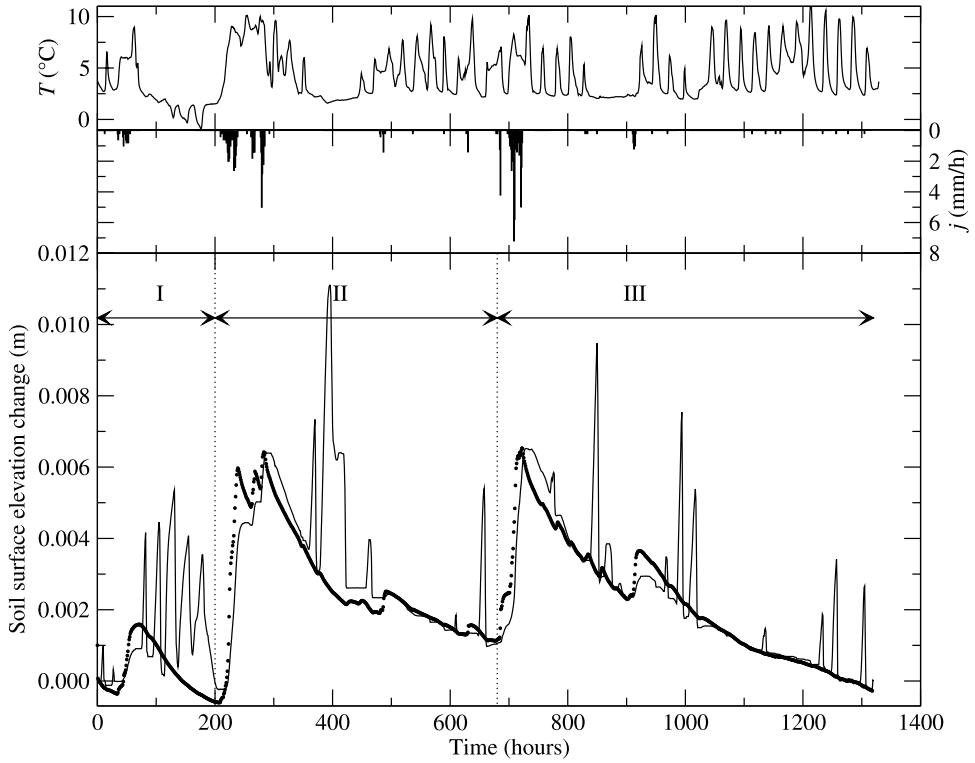

Figure 5. (top) Soil temperature T measured at 0.01 m and (middle) atmospheric forcing rate j over the time period covered by the simulation. The contribution due to evapotranspiration is on the average three orders of magnitude smaller than the maximum rainfall. (bottom) Comparison between the measured (solid lines) and simulated (dots) ground displacements.

The parameter combination that provides the best global fit is $K_s = 3.0 \times 10^{-7}$ m/s, $\delta_{sur} = 0.35$, $\lambda = 0.10$ m^{-1}. With these values the calculated Willmott parameters are equal to $\overline{d}_\psi = 0.91$ and $d_* = 0.81$. Table 1 summarizes the values of all the input parameters used by the model.

[27] Figure 4 shows that the range of variability of the computed retention curves at 0.15 m for the minimum and maximum values of ϕ as calculated during the simulation of the entire period spans the interval deduced from the field measurements. Note that the shapes of these curves, obtained for the shallowest partially decomposed peat, are in good agreement with those used in the hydrological parameterization of sapric histosols in the Canadian Land Surface Scheme (CLASS) [*Letts et al.*, 2000]. Similar retention curves are given by *Weiss et al.* [1998]. Moreover, the calibrated K_s is consistent with the range 10^{-6}–10^{-7} m/s provided by the Environmental Protection Agency of the Veneto Region (ARPAV) for the peat soils in the Venice Lagoon area [*ARPAV*, 2005]. The parameter δ is computed from the calibrated δ_{sur} and λ parameters and ranges between 0.35 at the top and 0.50 at the bottom of the peat column. These values correspond to a shrinkage geometry factor that remains always strictly smaller than 3. According to the basic model assumption, this implies an anisotropic three-dimensional deformation with a prevailing vertical component.

4.2. Comparison Between Simulated and Observed Results

[28] Figure 5 compares the measured and the simulated land displacements. The simulation results during the validation period (after 680 hours) show that the soil dynamics are well captured. The abrupt swelling peaks, clearly visible in the measured profile, are related to soil temperature approaching the freezing point and are not taken into account by the model. These sudden expansions, that typically occur in cold winter nights, are completely reversible and quickly dissipate in the morning when temperature increases [*Teatini et al.*, 2004]. During the calibration phase, the value of d_* from equation (23) has been computed after filtering out all these peaks from the data.

[29] The time evolution of the pressure head measured at depths of 0.15, 0.30, 0.45, and 0.60 m is compared in Figure 6 with the results provided by the model in the nodes located in the central vertical line of the mesh. The recorded profiles are affected by an uncertainty estimated in ±0.05 m, a value that is related to the length of the porous cups and the actual depth of insertion of the tensiometer tube. The latter uncertainty cannot be neglected as usually done in more conventional stronger suction soil situations. The agreement between experimental and computed values is satisfactory, with the simulated pressure heads that fall almost entirely within the uncertainty range of the observations. The dynamics of the event is particularly well captured.

[30] Predicted volumetric water content at 0.10, 0.20, 0.30, and 0.45 m are shown in Figure 7. It must be recalled that a specific TDR calibration curve for Zennare peat is not available. Nonetheless, the choice of *Myllys and Simojoki*'s [1996] model allows for a reasonable reproduction of the θ dynamics, especially in the shallow unsaturated layers. The

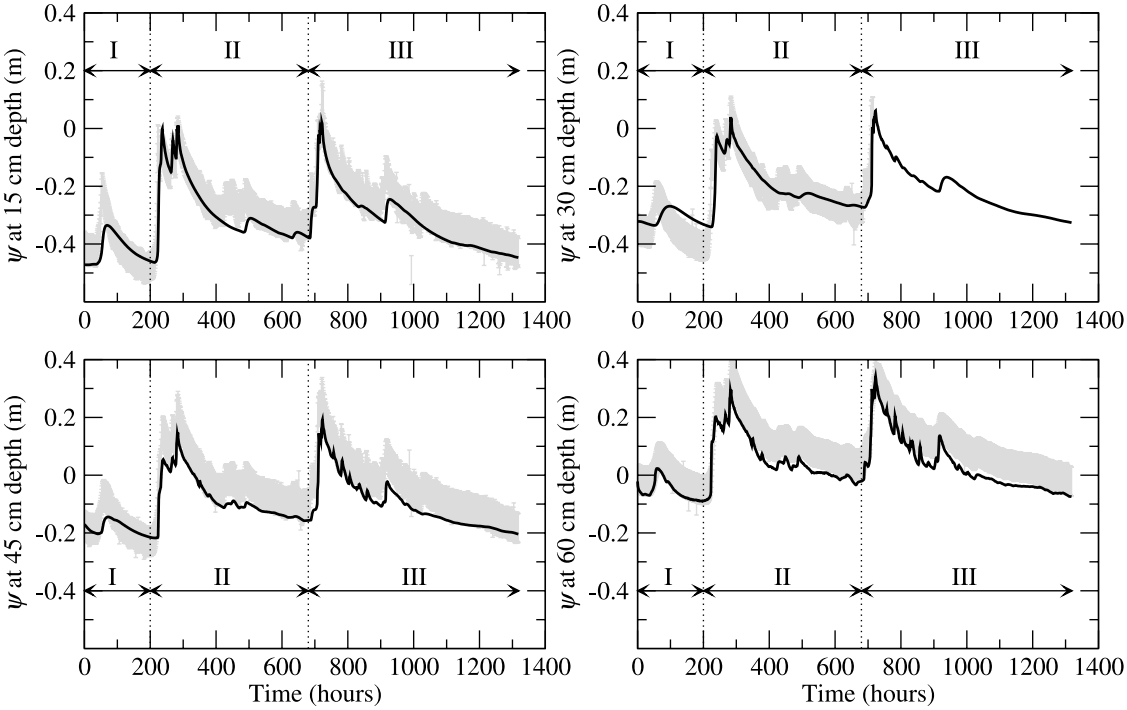

Figure 6. Comparison between measured (gray bars) and simulated (solid lines) pressure head profiles at various depths. The height of the bars is representative of the uncertainty (±0.05 m) of tensiometer measurements related to the ceramic cup length and to the actual installation depth of the sensors. The latter uncertainty cannot be neglected as usually done in more conventional stronger suction soil situations. The 0.30 m deep tensiometer stopped working soon after the second main rainfall event (at about 700 hours).

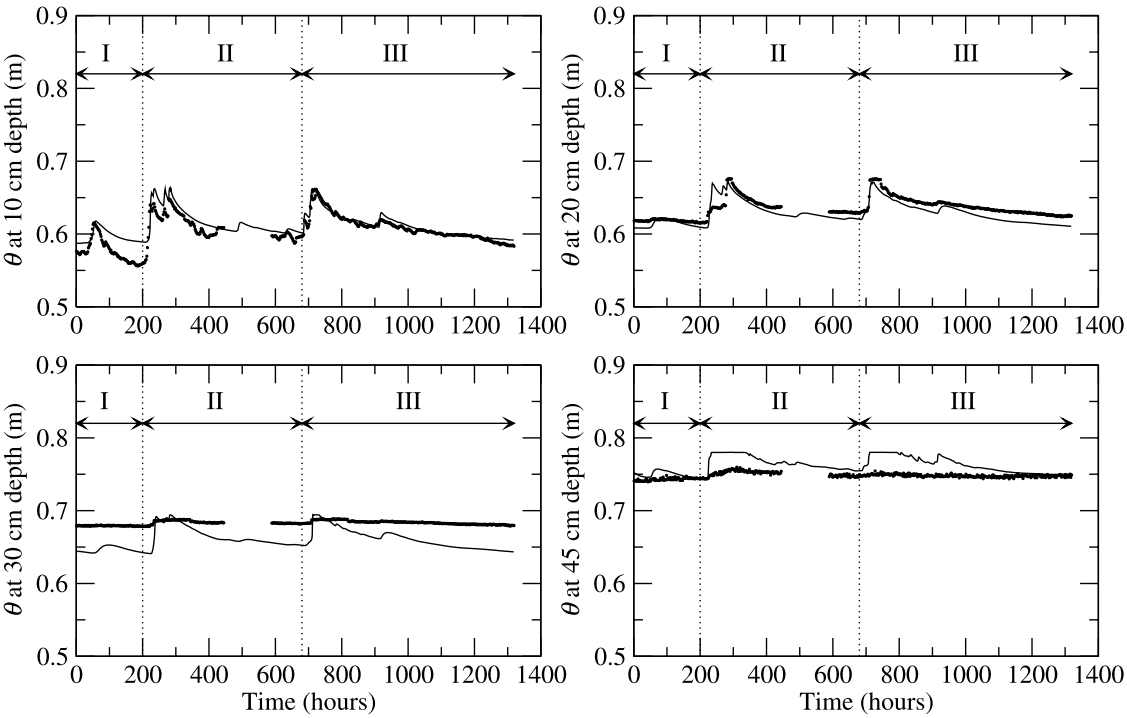

Figure 7. Comparison between measured (dots) and simulated (solid lines) water content at various depths. The measured values are estimated from TDR records according to *Myllys and Simojoki* [1996]. TDR probes did not work from ≈450 to ≈600 hours.

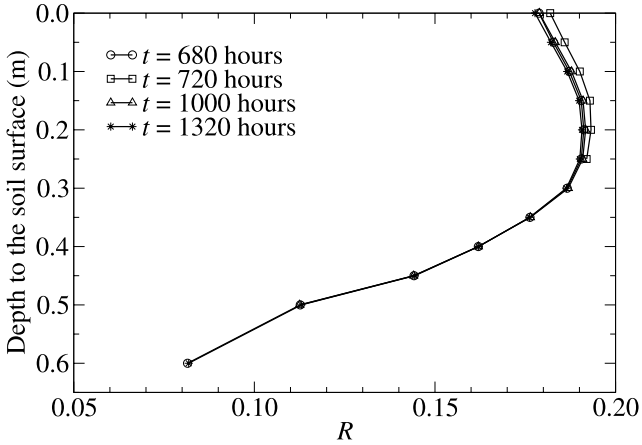

Figure 8. Computed profiles of the ratio $R = (S_w S_{uns})/(\phi \partial S_w/\partial \psi)$ versus depth for t = 680, 720, 1000, 1320 hours. In the saturated zone R is not defined. The profiles are relatively insensitive to time variations and show that the term $S_w S_{uns}$ cannot be neglected.

simulated time series of θ is a subdued replica of θ variability at shallower locations, while the measured water content displays little variations. The differences are more evident at 0.30 m. In fact the model retention curve, which is constant with depth, was calibrated using the data at 0.15 m only. Looking at Figure 4 we observe that the retention curves at depths greater than 0.15 m display a much smaller variability of the water content which, if taken into account in the model, would result in smoother oscillations of θ. However, the numerical code currently does not account for vertical variability of the retention curves.

[31] A specific analysis has been carried out to assess the relative importance of the swelling/shrinking process on the evaluation of the general storage term σ in the unsaturated zone. Figure 8 shows the ratio R defined as

$$R = \frac{S_w S_{uns}}{\phi \dfrac{\partial S_w}{\partial \psi}} = \frac{\delta (e S_w + 1)^{-1}}{1 - (\vartheta_0 + 1)^{1-\delta} \delta (e S_w + 1)^{\delta - 1}}, \qquad (24)$$

and computed by the model at each node of the mesh along the central vertical profile. The ratio R measures the contribution of the effect due to swelling/shrinkage as compared to the term $\phi \partial S_w/\partial \psi$, that is usually considered as the only significant factor in unsaturated mineral soils. The time variability of R is not significant, while the contribution of $S_w S_{uns}$ is not negligible, ranging from 8 to almost 20% of $\phi \partial S_w/\partial \psi$. The contribution of swelling/shrinkage on peat water dynamics is thus important, affecting directly the storage capacity of peatlands. These results confirm previous findings by *Schlotzhauer and Price* [1999], despite the cropped peat in the Zennare Basin is more decomposed than the peat investigated by *Schlotzhauer and Price* [1999] in Québec (Canada).

4.3. Sensitivity of the Proposed Swelling/Shrinkage Model

[32] A sensitivity analysis has been carried out to investigate the robustness of the proposed swelling/shrinkage model and to evaluate the influence of the parameters that exert the strongest control on peat hydrology and soil surface displacements. The variability of the threshold moisture ratio ϑ_0 has been initially investigated. Sapric decomposed peats have a higher bulk density and a lower water content than hemic or fibric undecomposed peats [*Letts et al.*, 2000]. Hence the former soil type is characterized by a lower ϑ_0 than the other two. Six different profiles for ϑ_0 as a function of depth have been considered. A profile typical of a boreal uncultivated peatland is derived by evaluating ϑ_0 from porosity data obtained from the CLASS parameterization [*Letts et al.*, 2000] (denoted by "CLASS" in Figure 9). The other limiting case is given by the ϑ_0 values evaluated from moisture content measurements at the Zennare field site ("Best fit" in Figure 9). Four intermediate profiles ("Profile 1" to "Profile 4" in Figure 9) were also employed in the analysis. The sensitivity to δ_{sur} and λ is performed ensuring that δ of equation (22) lies always within its interval of definition (1/3–1.0).

[33] The results of the analysis show that the sensitivity of the model to variations of the ϑ_0 profile is negligible for pressure head, while is significant if looking at the volumetric water content. Note that in our simulations, the depth of the saturated zone is primarily controlled by the boundary

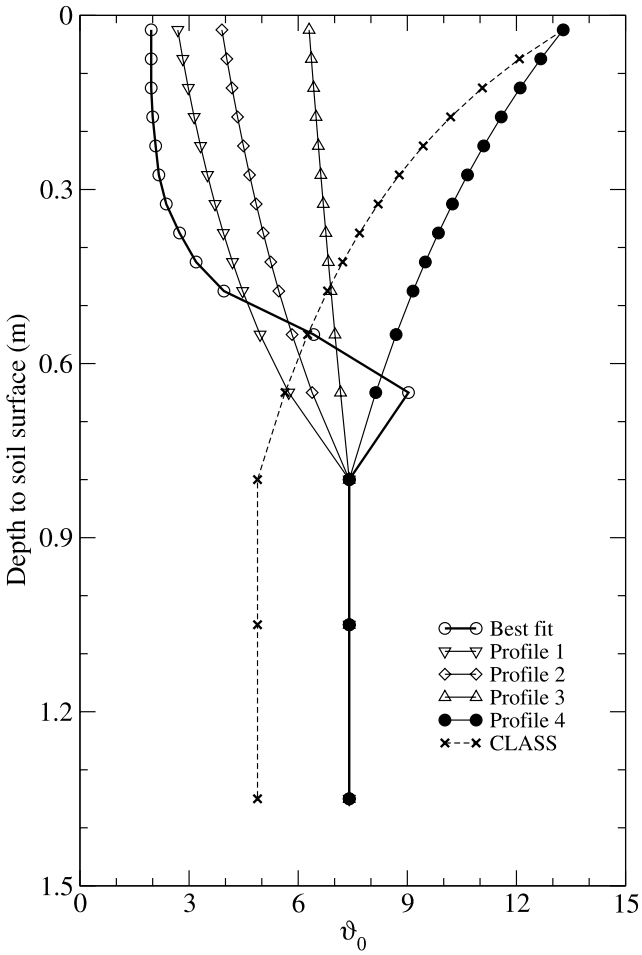

Figure 9. Behavior of ϑ_0 versus depth as used in the sensitivity analysis, compared with the profile derived from the CLASS parameterization [*Letts et al.*, 2000].

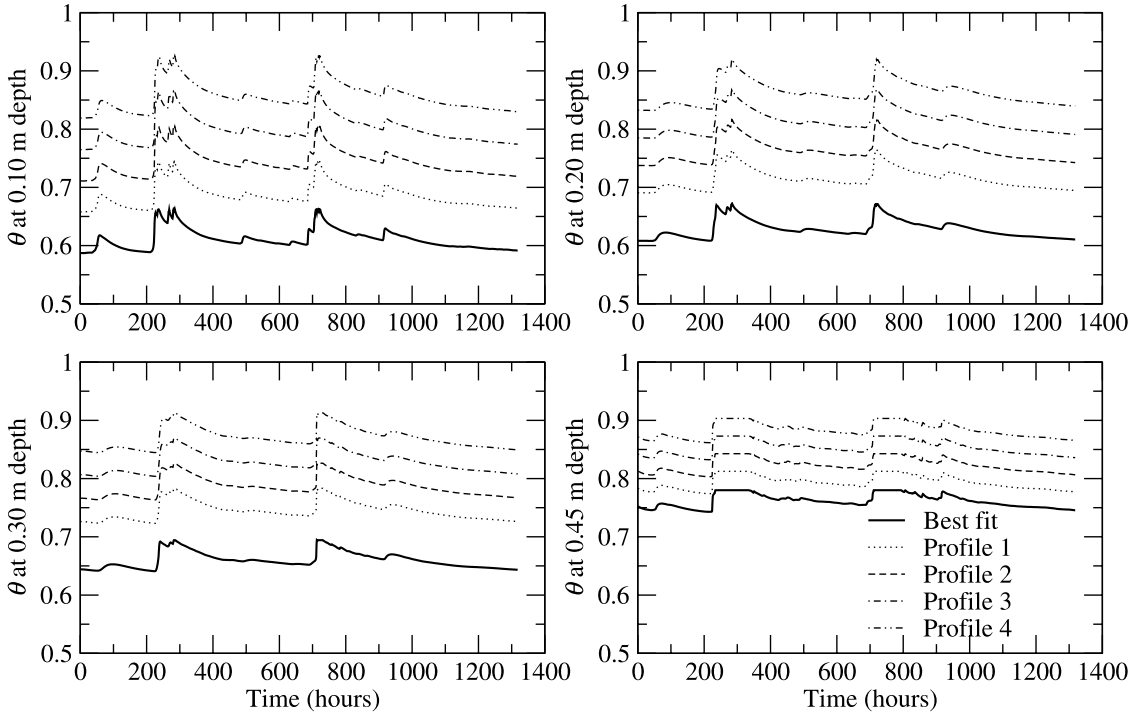

Figure 10. Effect of ϑ_0 variations on the computed volumetric content at various depths.

conditions and not by the atmospheric fluxes, and thus it is not sensitive to variations of the soil parameters. The water content curves are shifted by a positive quantity in going from the "Best fit" to "Profile 4", as shown in Figure 10, while the dynamics of the process is the same for all the profiles.

[34] The influence of the shrinking/swelling parameters δ_{sur}, ϑ_0 and λ on the computed soil surface displacements is shown in Figures 11, 12, and 13, respectively. The model is highly sensitive to variations of δ_{sur} and the nonlinearity of equation (8) is shown by the fact that a doubled value of δ_{sur} produces an increase of the surface displacements by a factor of around four. The sensitivity to ϑ_0 is not as important, mainly resulting in a shift of the displacement curves. The influence of λ on the displacements is similar, but less pronounced, with respect to that of δ_{sur}. The main differences can be detected in the swelling peak increase, which is reduced by one order of magnitude compared to the effect of δ_{sur}, and in a faster shrinkage dynamics during the drainage periods.

[35] The robustness of the proposed model is evaluated also by means of a simulation which employs the "CLASS" ϑ_0 profile together with the parameters of the van Genuchten retention curve calculated by the CLASS parameterization (n = 1.90 and ψ_s = −0.12 m). The results show a soil surface displacement of the order of 0.10 m, in agreement with values observed in Canadian uncultivated peatlands [*Price and Schlotzhauer*, 1999].

5. Conclusions

[36] A new model for reversible peat displacements related to soil moisture variations has been derived by

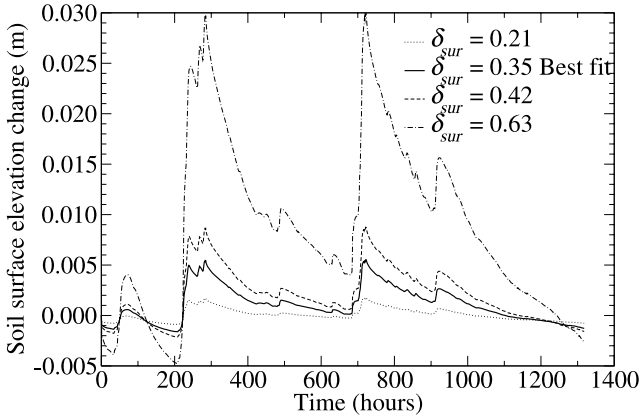

Figure 11. Effect of δ_{sur} variations on the computed soil surface displacements.

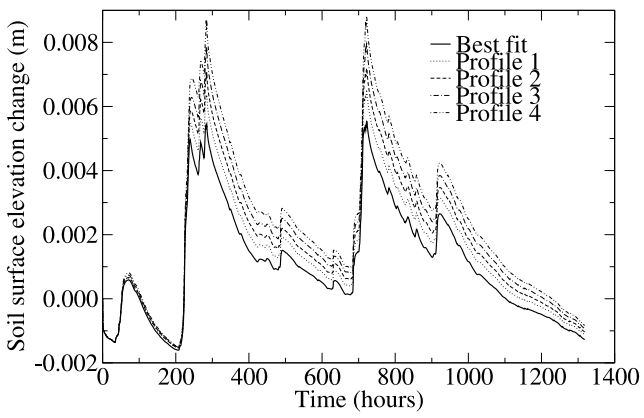

Figure 12. Effect of ϑ_0 variations on the computed soil surface displacements.

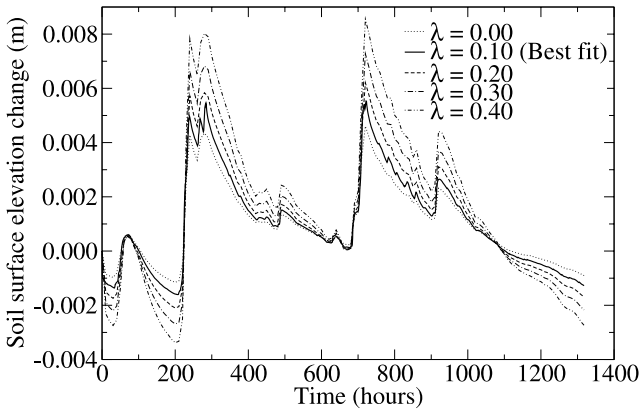

Figure 13. Effect of λ variations on the computed soil surface displacements.

considering three-dimensional anisotropic deformations in unsaturated conditions. The void ratio is related to the moisture ratio by means of a physically based constitutive relationship that takes into account the nonlinearity of the soil deformation in the unsaturated zone. The model employs only two parameters that can be easily calibrated from observed data. Our shrinkage characteristic curve has been validated by comparison against an extensive data set of published laboratory experiments performed on peat samples.

[37] The constitutive relationship has been implemented in Richards' equation through a suitable modification of the general storage term, to consider a porosity that varies with water saturation. A finite element code based on this modified formulation has been applied for the simulation of a drained cropped peatland, for which a large field data set of hydrological quantities is available. The application of the model shows a satisfactory match between measured and simulated soil surface displacements, with values of the estimated and calibrated soil parameters in good agreement with others found in the literature and through local surveys. Also the pressure head and water content dynamics are well captured. A sensitivity analysis shows that the proposed swelling/shrinkage model is robust to changes of most of the defining parameters. The contribution of the new developed term in the flow equation cannot be neglected, especially as regards peat water storage capacity, confirming that swelling/shrinkage process must be taken into account in the management of drained cropped peatlands.

[38] New developments are in progress by simulating a two-dimensional field section, in order to investigate the accuracy of the model in more truthful, less constrained conditions. We will also address the effects of the saturated zone, neglected in this study, on the total soil surface deformation when relevant field data will become available.

Notation

d Willmott index of agreement.
$\overline{d}_{\psi}$ Willmott index of agreement for ψ profiles.
d_* Willmott index of agreement for peat surface displacements.
D height of the discretized peat column, m.
e void ratio.
ℓ height of the peat volume, m.
ℓ_0 height of the peat volume at saturation or inception of cracks, m.
ℓ_i initial height of the peat volume, m.
ℓ' horizontal dimension of the peat volume, m.
ET_0 reference evapotranspiration, m/s.
K_b bulk dielectric permittivity.
K_r relative hydraulic conductivity.
K_s saturated hydraulic conductivity, m/s.
m fitting parameter in the van Genuchten retention curve.
M_s mass of solids, kg.
M_w mass of water, kg.
n fitting parameter in the van Genuchten retention curve.
$\overline{O}$ mean of O_i.
O_i observed values in the computation of d.
P_i predicted values in the computation of d.
q source or sink term in Richards' equation, s^{-1}.
r_s shrinkage geometry factor.
R ratio between $S_w S_{uns}$ and $\phi \partial S_w / \partial \psi$.
S_s elastic storage coefficient for soils in saturated conditions, m^{-1}.
S_{uns} elastic storage coefficient for peat in partially saturated conditions, m^{-1}.
S_w water saturation.
S_{we} effective water saturation.
S_{wr} residual water saturation.
t time, s.
v specific volume of peat, m^3/kg.
v_0 specific volume of peat at saturation or inception of cracks, m^3/kg.
v_i initial specific volume of peat, m^3/kg.
v_s specific volume of solids, m^3/kg.
v_w specific volume of water, m^3/kg.
v^* specific volume of peat layer, m^3/kg.
V volume of peat, m^3.
V_s volume of solids, m^3.
V_v volume of voids, m^3.
V_w volume of water, m^3.
z vertical spatial coordinate, m.
α exponent of the relationship between horizontal and vertical deformation.
δ inverse of r_s.
δ_{sur} value of δ at the peat surface.
ε_h horizontal deformation.
ε_v vertical deformation.
ϑ moisture ratio.
ϑ_0 threshold moisture ratio.
θ volumetric water content.
θ_0 threshold volumetric water content.
θ_r residual volumetric water content.
Θ gravimetric water content.
Θ_0 gravimetric water content at saturation or inception of cracks.
Θ_i initial gravimetric water content.
λ slope of the $\delta(z)$ relationship, m^{-1}.
ϕ porosity.
σ general storage term, m^{-1}.
ψ pressure head, m.

ψ_s fitting parameter in the van Genuchten retention curve, m.

∇ spatial gradient operator, m^{-1}.

[39] **Acknowledgments.** This work has been partially supported by Co.Ri.La., Consorzio di Bonifica Adige-Bacchiglione, Municipalities of Cavarzere, Chioggia and Cona (Venice-Italy), Servizio Informativo del Magistrato alle Acque per la Laguna di Venezia, and the University of Padova project entitled "Multiscale monitoring of CO_2 fluxes from agricultural soils and modeling of the spatial variability of the sources for quantification and control of emission into the atmosphere." We gratefully acknowledge Claudio Paniconi (INRS-ETE, University of Québec), whose comments on early versions of the manuscript were valuable, and Ryszard Oleszczuk (Warsaw Agricultural University) for kindly providing the experimental data of Figure 2.

References

Allen, R. G., L. S. Pereira, D. Raes, and M. Smith (1998), Crop evapotranspiration—Guidelines for computing crop water requirements, *Irrig. Drain. Pap.*, *56*.

Environmental Protection Agency of the Veneto Region (ARPAV) (2005), Carta dei suoli del Veneto, Venice, Italy.

Bixio, A. C., S. Orlandini, C. Paniconi, and M. Putti (2000), Physically-based distributed model for coupled surface runoff and subsurface flow simulation at the catchment scale, in *Computational Methods in Water Resources XIII*, vol. 2, edited by L. Bentley et al., pp. 1093–1099, A. A. Balkema, Brookfield, Vt.

Bronswijk, J. J. B. (1988), Modeling of water balance, cracking and subsidence of clay soils, *J. Hydrol.*, *97*, 199–212.

Bronswijk, J. J. B. (1990), Shrinkage geometry of a heavy clay soil at various stresses, *Soil Sci. Soc. Am. J.*, *54*, 1500–1502.

Brooks, R. H., and A. T. Corey (1964), Hydraulic properties of porous media, *Hydrol. Pap. 3*, Colo. State Univ., Fort Collins.

Camporese, M. (2006), Modeling and experimental analysis of peat hydrology and its relationships with the subsidence of the Zennare Basin, Venice (Italy), Ph.D. thesis, Univ. degli Studi di Padova, Padua, Italy.

Camporese, M., M. Putti, P. Salandin, and P. Teatini (2004), Modeling peatland hydrology and related elastic deformation, in *Computational Methods in Water Resources XV*, vol. 1, edited by C. Miller et al., pp. 1453–1465, Elsevier, New York.

Dasberg, S., and S. P. Neuman (1977), Peat hydrology in the Hula Basin, Israel: I. Properties of peat, *J. Hydrol.*, *32*, 219–239.

Deverel, S. J., and S. Rojstaczer (1996), Subsidence of agricultural lands in the Sacramento–San Joaquin Delta, California: Role of aqueous and gaseous carbon fluxes, *Water Resour. Res.*, *32*(8), 2359–2367.

Fornasiero, A., M. Putti, P. Teatini, S. Ferraris, F. Rizzetto, and L. Tosi (2003), Monitoring of hydrological parameters related to peat oxidation in a subsiding coastal basin south of Venice, Italy, in *Hydrology of the Mediterranean and Semiarid Regions*, edited by E. Servat et al., *IAHS Publ.*, *278*, 458–462.

Galloway, D., D. R. Jones, and S. E. Ingebritsen (1999), Land subsidence in the United States, *U.S. Geol. Surv. Circ.*, *1182*.

Gambolati, G. (1974), Second-order theory of flow in three-dimensional deforming media, *Water Resour. Res.*, *10*(6), 1217–1228.

Gambolati, G., M. Putti, P. Teatini, M. Camporese, S. Ferraris, G. Gasparetto Stori, V. Nicoletti, F. Rizzetto, S. Silvestri, and L. Tosi (2005), Peatland oxidation enhances subsidence in the Venice watershed, *Eos Trans. AGU*, *86*(23), 217–224.

Gambolati, G., M. Putti, P. Teatini, and G. Gasparetto Stori (2006), Subsidence due to peat oxidation and impact on drainage infrastructures in a farmland catchment south of the Venice Lagoon, *Environ. Geol.*, *49*, 814–820.

Gatti, P., M. Bonardi, L. Tosi, F. Rizzetto, A. Fornasiero, G. Gambolati, M. Putti, and P. Teatini (2002), The peat deposit of the subsiding Zennare Basin, south of the Venice Lagoon, Italy: Geotechnical classification and preliminary mineralogical characterization, in *Scientific Research and Safeguarding of Venice (CORILA Research Program 2001 Results)*, edited by P. Campostrini, pp. 241–257, Ist. Veneto di Sci. Lett. ed Arti, La Garangola, Padua, Italy.

Glaser, P. H., J. P. Chanton, P. Morin, D. O. Rosenberry, D. I. Siegel, O. Ruud, L. I. Chasar, and A. S. Reeve (2004), Surface deformations as indicators of deep ebullition fluxes in a large northern peatland, *Global Biogeochem. Cycles*, *18*, GB1003, doi:10.1029/2003GB002069.

Hendriks, R. F. A. (2004), An analytical equation for describing the shrinkage characteristic of peat soils, in *Wise Use of Peatlands, Proceedings of the 12th International Peat Congress*, edited by J. Päivänen, pp. 1343–1348, Int. Peat Soc., Jyväskylä, Finland.

Hobbs, N. B. (1986), Mire morphology and the properties and behaviour of some British and foreign peats, *Q. J. Eng. Geol.*, *19*, 7–80.

Ingram, H. A. P. (1983), Hydrology, in *Mires: Swamp, Bog, Fen, and Moor*, edited by A. J. P. Gore, pp. 67–158, Elsevier, New York.

Kellner, E., J. M. Waddington, and J. S. Price (2005), Dynamics of biogenic gas bubbles in peat: Potential effects on water storage and peat deformation, *Water Resour. Res.*, *41*, W08417, doi:10.1029/2004WR003732.

Kennedy, G. W., and J. S. Price (2004), Simulating soil water dynamics in a cutover bog, *Water Resour. Res.*, *40*, W12410, doi:10.1029/2004WR003099.

Kennedy, G. W., and J. S. Price (2005), A conceptual model of volume-change controls on the hydrology of cutover peats, *J. Hydrol.*, *302*(1–4), 13–27.

Letts, M. G., N. T. Roulet, N. T. Comer, M. R. Skarupa, and D. L. Verseghy (2000), Parametrization of peatland hydraulic properties for the Canadian Land Surface Scheme, *Atmos. Ocean*, *38*(1), 141–160.

Myllys, M., and A. Simojoki (1996), Calibration of time domain reflectometry (TDR) for soil moisture measurements in cultivated peat soils, *Suo*, *47*, 1–6.

Oleszczuk, R., K. Bohne, J. Szatylowicz, T. Brandyk, and T. Gnatowski (2003), Influence of load on shrinkage behavior of peat soils, *J. Plant Nutr. Soil Sci.*, *166*, 220–224.

Paniconi, C., and M. Putti (1994), A comparison of Picard and Newton iteration in the numerical solution of multidimensional variably saturated flow problems, *Water Resour. Res.*, *30*(12), 3357–3374.

Philip, J. R. (1969), Hydrostatics and hydrodynamics in swelling soils, *Water Resour. Res.*, *5*(5), 1070–1077.

Price, J. S. (2003), Role and character of seasonal peat soil deformation on the hydrology of undisturbed and cutover peatlands, *Water Resour. Res.*, *39*(9), 1241, doi:10.1029/2002WR001302.

Price, J. S., and S. M. Schlotzhauer (1999), Importance of shrinkage and compression in determining water storage changes in peat: The case of a mined peatland, *Hydrol. Processes*, *13*, 2591–2601.

Price, J. S., and G. S. Whitehead (2001), Developing hydrologic thresholds for Sphagnum recolonization on an abandoned cutover bog, *Wetlands*, *21*, 32–40.

Putti, M., and C. Paniconi (2004), Time step and stability control for a coupled model of surface and subsurface flow, in *Computational Methods in Water Resources XV*, vol. 1, edited by C. Miller et al., pp. 1391–1402, Elsevier, New York.

Pyatt, D. G., and A. L. John (1989), Modelling volume changes in peat under conifer plantations, *J. Soil Sci.*, *40*, 695–706.

Schlotzhauer, S. M., and J. S. Price (1999), Soil water flow dynamics in a managed cutover peat field, Quebec: Field and laboratory investigation, *Water Resour. Res.*, *35*(12), 3675–3683.

Schothorst, C. J. (1977), Subsidence of low moor peat soils in the western Netherlands, *Geoderma*, *17*, 265–291.

Smiles, D. E. (2000), Hydrology of swelling soils: A review, *Aust. J. Soil Res.*, *38*, 501–521.

Teatini, P., M. Putti, G. Gambolati, S. Ferraris, and M. Camporese (2004), Reversible/irreversible peat surface displacements and hydrological regime in the Zennare Basin, Venice, in *Scientific Research and Safeguarding of Venice (CORILA Research Program 2001–2003, 2002 Results)*, edited by P. Campostrini, pp. 93–106, La Garangola, Venice, Italy.

Terzaghi, K. (1943), *Theoretical Soil Mechanics*, John Wiley, Hoboken, N. J.

Topp, G. C., J. L. Davis, and A. P. Annan (1980), Electromagnetic determination of soil water content: Measurements in coaxial transmission lines, *Water Resour. Res.*, *16*(3), 574–582.

Van den Akker, J. J. H., and R. F. A. Hendriks (1997), Shrinkage characteristics of Dutch peat soils, in *Proceedings International Congress "Peat in Horticulture—Its Use and Sustainability*, edited by G. Schmilewski, pp. 156–182, Int. Peat Soc., Jyskä, Finland.

van Genuchten, M. T. (1980), A closed-form equation for predicting the hydraulic conductivity of unsaturated soils, *Soil Sci. Soc. Am. J.*, *44*, 892–898.

Weiss, R., J. Alm, R. Laiho, and J. Laine (1998), Modeling moisture retention in peat soils, *Soil Sci. Soc. Am. J.*, *62*(2), 305–313.

Willmott, C. (1948), On the evaluation of model performance in physical geography, in *Spatial Statistics and Models*, edited by G. Gaille and C. Willmott, pp. 443–460, Springer, New York.

Wösten, J. H. M., A. B. Ismail, and A. L. M. van Wijk (1997), Peat subsidence and its practical implications: A case study in Malaysia, *Geoderma*, *78*, 25–36.

M. Camporese, INRS-ETE, University of Quebec, 490, de la Couronne, Quebec, QC, Canada G1K 9A9. (matteo_camporese@ete.inrs.ca)

S. Ferraris, Department of Agricultural, Forest, and Environmental Economics and Engineering, University of Turin, Via Da Vinci 44, I-10095 Grugliasco (TO), Italy. (stefano.ferraris@unito.it)

M. Putti and P. Teatini, Department of Mathematical Methods and Models for Scientific Applications, University of Padua, Via Belzoni 7, I-35131 Padua, Italy. (putti@dmsa.unipd.it; teatini@dmsa.unipd.it)

P. Salandin, Department of Hydraulic, Maritime, Environmental, and Geotechnical Engineering, University of Padua, Via Loredan 20, I-35131 Padua, Italy. (sala@idra.unipd.it)